



Structure and magnetic properties of RNi (R = Gd, Tb, Dy, Sm) and $R_6M_{1.67}Si_3$ (R = Ce, Gd, Tb; M = Ni, Co) hydrides

Yu.L. Yaropolov^{a,*}, A.S. Andreenko^a, S.A. Nikitin^a, S.S. Agafonov^b, V.P. Glazkov^b, V.N. Verbetsky^a

^a Moscow State University, GSP-3, Leninskie Gory, Moscow 119992, Russia

^b Russian Research Centre Kurchatov Institute, 1, Kurchatov Sq., Moscow 123182, Russia

ARTICLE INFO

Article history:

Received 29 July 2010

Received in revised form 5 January 2011

Accepted 7 January 2011

Available online 14 January 2011

Keywords:

Rare earth alloys and compounds

Metal hydrides

Magnetization

Crystal structure

Magnetic measurements

Neutron diffraction

ABSTRACT

The paper reports the influence of hydrogen absorption on the structure and magnetic properties of intermetallic compounds RNi (R = Gd, Tb, Dy, Sm) and $R_6M_{1.67}Si_3$ (R = Ce, Gd, Tb; M = Ni, Co). It is demonstrated that the ternary hydrides GdNiH_{3.2}, TbNiH_{3.4}, DyNiH_{3.4}, and SmNiH_{3.7} have similar CrB-type orthorhombic structures. In the structures of TbNiD_{3.4} and DyNiD_{3.4}, deuterium atoms occupy tetrahedral 8f-interstices [R₃Ni], trigonal bipyramidal 4c-interstices [R₃Ni₂], and octahedral 4b-interstices [R₄Ni₂]. The hydrides of $R_6M_{1.67}Si_3$ retain the hexagonal structure of their parent compound. In the structures of Tb₆Co_{1.67}Si₃D_{11.2} and Ce₆Ni_{1.67}Si₃D_{12.3}, deuterium atoms occupy tetrahedral 4f-interstices [R₃M] and two types of tetrahedral interstices [R₃Si]: 12i₁ and 12i₂. The formation of the hydrides causes a substantial expansion of the metallic sublattice, a weakening of ferromagnetic interactions, and a decrease in the magnetic transition temperature.

© 2011 Elsevier B.V. All rights reserved.

1. Introduction

Intermetallic compounds (IMCs) containing rare earth metal atoms have attracted considerable attention due to their high potential for various applications. Considerable attention has recently been focused on magnetocaloric materials used in magnetic refrigeration. After the observation of a giant magnetocaloric effect in Gd₅Si₂Ge₂ [1], interest in IMCs containing gadolinium and other rare earth metals has increased.

The magnetic properties of an IMC depend on the strength of the exchange interactions between magnetic atoms, which is determined by the interatomic distances and electronic structure. The introduction of hydrogen atoms into an IMC usually results in significant changes in its crystal and electronic structure [2–5]. Different types of exchange interactions are possible in compounds consisting of rare earth and 3d transition elements: indirect exchange between the 4f-subshells of the rare earth ions through the conduction electrons and 3d-electrons, and direct exchange interaction between the 3d-electrons. The strength of these interactions depends on the distances between the interacting atoms and, therefore, on the geometrical parameters of the crystal lattice. Lattice expansion causes not only an increase in the interatomic distances, but also a change in the electronic structure and redi-

tribution of the electron density in the bulk of the crystal lattice, thus exerting a direct effect on the magnetism of the 3d-ions. Incorporating into the IMC structure, hydrogen can partially donate its electron to the conduction band or, conversely, acquire a partial negative charge H^{δ-}. The change in the number of electrons in the conduction band leads to a change in the electron density at the Fermi level, and this produces a direct effect on the magnetic properties of the compound. When hydrogen acts as an electron donor, it increases the electron density in the conduction band, which is responsible for the exchange interaction. This leads to an increase in the magnetization and Curie temperature of the compound. If hydrogen partially withdraws electron density from the conduction band, the magnetization and Curie temperature of the hydride decrease. Thus, the effect of hydrogenation on the structural and magnetic properties of IMCs is of considerable interest.

Rare-earth intermetallics possess promising magnetic properties due to the large magnetic moments of the rare earth atoms. The RNi and $R_6M_{1.67}Si_3$ IMC series attracted our attention because they have approximately equal atomic ratios of the “hydridable” rare earth element to the “nonhydridable” transition elements. In addition, these compounds react readily with hydrogen at room temperature and relatively low hydrogen pressures. Finally, both IMC series show a strong magnetocaloric effect near the magnetic transition temperatures [6–9].

The magnetic properties of the RNi compounds and their hydrides were investigated previously between 78 and 300 K [10]. The magnetic transition temperatures of the RNi compounds and

* Corresponding author. Tel.: +7 495 939 1413; fax: +7 495 932 8846.
E-mail address: yaropolov@inbox.ru (Yu.L. Yaropolov).

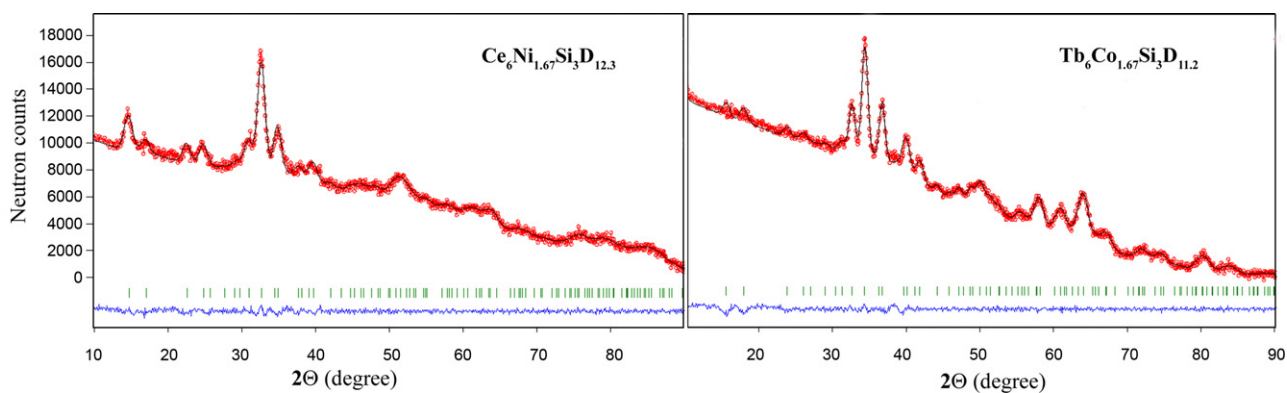


Fig. 1. Neutron powder diffraction patterns of $\text{Ce}_6\text{Ni}_{1.67}\text{Si}_3\text{D}_{12.3}$ and $\text{Tb}_6\text{Co}_{1.67}\text{Si}_3\text{D}_{11.2}$.

all of their hydrides turned out to be below the nitrogen boiling point (~ 78 K). However, the calculated temperature dependences of the reciprocal susceptibilities are linear in the temperature range 78–300 K and obey the Curie–Weiss law $\chi = C/(T - \theta)$ in all cases except for SmNi and SmNiH_{3.7}. This makes it possible to estimate the paramagnetic Curie temperature θ_p and to calculate the effective magnetic moments μ_{eff} of the rare earth atoms.

Here, we report the effect of hydrogenation on the structural and magnetic properties of the RNi (R = Gd, Tb, Dy, Sm) and $\text{R}_6\text{M}_{1.67}\text{Si}_3$ (R = Ce, Gd, Tb; M = Ni, Co) compounds.

2. Experimental details

The intermetallic compounds RNi and $\text{R}_6\text{M}_{1.67}\text{Si}_3$ were synthesized by arc melting under an argon atmosphere in a furnace with a nonconsumable tungsten electrode and a water-cooled copper hearth. The starting components were nickel (99.99%), cobalt (99.99%), silicon (99.99%), and rare earth metals (99.9%), and titanium sponge was used as a getter. The amounts of rare earths in the stocks were chosen so as to compensate for the metal losses. The samples were turned over and remelted several times to ensure homogeneity.

The hydrides were synthesized in a Sieverts-type volumetric apparatus at room temperature and hydrogen pressures of up to 1 MPa. The composition of the resulting hydrides was derived from volumetric measurements using the van der Waals equation.

The phase composition and unit cell parameters of the starting alloys and their hydrides were determined by X-ray powder diffraction using $\text{Cu K}\alpha$ radiation. The RNi compounds were single-phase according to their X-ray diffraction patterns, while the $\text{R}_6\text{M}_{1.67}\text{Si}_3$ compounds contained more than 35% impurities. For this reason, these samples were annealed at 900 °C for 10 days in evacuated quartz tubes. As a result, the impurity content decreased to 5% or below.

Several deuterides were prepared by the same technique in order to study their structure by neutron powder diffraction. The neutron diffraction experiments were performed with the DISK diffractometer at Kurchatov Institute using neutrons with a wavelength of 1.668 Å.

Magnetization measurements were performed with 150–400 mg samples in the form of pellets (hydrides) or ingots (starting alloys) in the temperature range 78–300 K using a vibration magnetometer.

3. Results and discussion

3.1. Crystal structure of $\text{Tb}_6\text{Co}_{1.67}\text{Si}_3\text{D}_{11.2}$ and $\text{Ce}_6\text{Ni}_{1.67}\text{Si}_3\text{D}_{12.3}$

According to the X-ray diffraction data, the $\text{R}_6\text{M}_{1.67}\text{Si}_3$ compounds have $\text{Ce}_6\text{Ni}_2\text{Si}_3$ -type hexagonal structures, space group $P6_3/m$, with the unit cell parameters close to those reported previously [11–15]. The metal lattices of the hydride phases were of the same structure type as the virgin IMCs, but a pronounced anisotropic distortion of the unit cell was nevertheless observed: the lattice was expanded along the *x* and *y* crystallographic axes and contracted along the *z* axis (Table 1).

X-ray and neutron powder diffraction studies were performed for $\text{Tb}_6\text{Co}_{1.67}\text{Si}_3\text{D}_{11.2}$ and $\text{Ce}_6\text{Ni}_{1.67}\text{Si}_3\text{D}_{12.3}$. The neutron data (Fig. 1) were used to refine the atomic coordinates and occupancies of the sites filled with deuterium atoms (Table 1). A crystallographic

analysis of the $\text{Ce}_6\text{Ni}_2\text{Si}_3$ -type structure showed that hydrogen atoms could occupy only $[\text{R}_3\text{T}]$ and $[\text{R}_2\text{T}_2]$ tetrahedral interstices (T = Ni, Co, Si) in its lattice. According to an empirical rule [16], the preferable interstices to be occupied by hydrogen are those surrounded by the maximum possible number of “hydridable” metal atoms. This means that the $[\text{R}_3\text{T}]$ tetrahedral interstices are most readily occupied by hydrogen atoms. In addition, the H–H distances must be longer than 1.2–2.0 Å, so hydrogen atoms will not occupy 12i- $[\text{R}_2\text{MSi}]$ interstices with a lower R content. For the same reason, only half the 4f- $[\text{R}_3\text{M}]$ and 6h- $[\text{R}_3\text{Si}]$ interstices, whose R_3 faces are in the (001) crystallographic plane, can be filled by hydrogen atoms, because the hydrogen atoms sitting on these sites block the adjacent sites of the same type. Moreover, the hydrogen atoms in the 4f- $[\text{R}_3\text{M}]$ and 6h- $[\text{R}_3\text{Si}]$ sites can partially block two types of $[\text{R}_3\text{Si}]$ interstices, namely, 12i₁ and 12i₂, whose R_3 faces are in another crystallographic plane (Fig. 2).

Based on these facts and the deuterium content calculated from volumetric data, we suggest a structural model in which deuterium atoms occupy half the 4f- $[\text{R}_3\text{M}]$ interstices and two types of the $[\text{R}_3\text{Si}]$ interstices: 12i₁ and 12i₂ (Fig. 3). Based on this structural model, the maximum deuterium content of the studied deuterides could be $\text{D}/\text{f.u.} = 13$.

According to the neutron diffraction data, the deuterium content of the deuterides corresponded to the formulas $\text{Tb}_6\text{Co}_{1.67}\text{Si}_3\text{D}_{11.2}$ and $\text{Ce}_6\text{Ni}_{1.67}\text{Si}_3\text{D}_{12.3}$. The introduction of deuterium atoms into the 4f sites results in a 5–6% increase in the R–R distances, while the

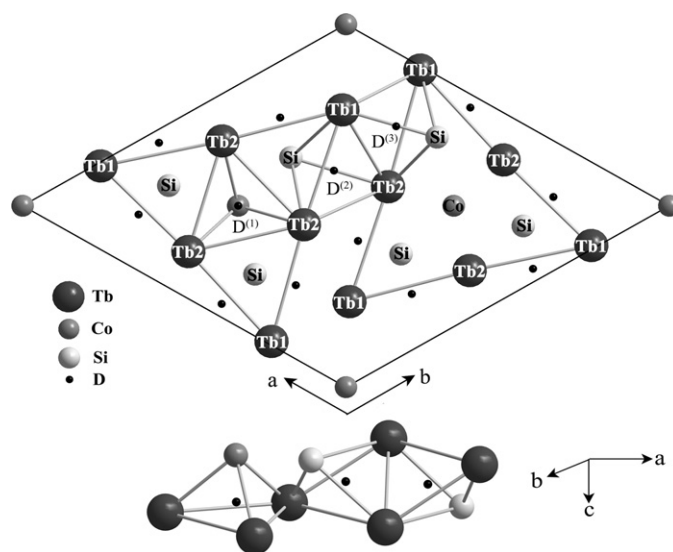


Fig. 2. $\text{Tb}_6\text{Co}_{1.67}\text{Si}_3\text{D}_{11.2}$ structure and coordination polyhedra of deuterium atoms.

Table 1
Refined structural parameters of $\text{Ce}_6\text{Ni}_{1.67}\text{Si}_3\text{D}_{12.3}$ and $\text{Tb}_6\text{Co}_{1.67}\text{Si}_3\text{D}_{11.2}$.

Compound	Atom	x	y	z	B_{iso}^* (\AA^2)	Occupancy
$\text{Ce}_6\text{Ni}_{1.67}\text{Si}_3\text{D}_{12.3}$ Space group $P6_3/m$ $a = 13.00(2)$ ($\Delta a/a_0 = 7.7\%$) $c = 4.134(3)$ ($\Delta c/c_0 = -4.1\%$) $V = 605.0(4)$ ($\Delta V/V_0 = 11.3\%$) $R_{\text{Bragg}} = 2.11$, $R_{\text{F}} = 2.42$	$\text{Ce}^{(1)}\text{-6h}$	0.242(2)	0.230(2)	1/4	1.26	1
	$\text{Ce}^{(2)}\text{-6h Ni}^{(1)}\text{-4e}$	0.513(4)	0.130(1)	1/4	1.96	1
	$\text{Ni}^{(2)}\text{-2c}$	0	0	0.081(1)	1.11	0.25(5)
	$\text{Ni}^{(3)}\text{-2a}$	1/3	2/3	1/4	0.61	1
	Si-6h	0	0	1/4	1.27	0.21(6)
	$\text{D}^{(1)}\text{-4f}$	0.170(1)	0.452(5)	1/4	2.10	1
	$\text{D}^{(2)}\text{-12i}_1$	1/3	2/3	0.609(6)	3.01	0.48(2)
	$\text{D}^{(3)}\text{-12i}_2$	0.420(5)	0.394(4)	0.504(4)	2.45	0.96(5)
		0.207(1)	0.350(3)	0.495(4)	2.53	0.93(7)
		0.238(1)	0.228(2)	1/4	0.87	1.0
		0.511(3)	0.130(1)	1/4	1.02	1.0
$\text{Tb}_6\text{Co}_{1.67}\text{Si}_3\text{D}_{11.2}$ Space group $P6_3/m$ $a = 12.353(7)$ ($\Delta a/a_0 = 5.9\%$) $c = 3.950(3)$ ($\Delta c/c_0 = -4.5\%$) $V = 522.0(3)$ ($\Delta V/V_0 = 6.7\%$) $R_{\text{Bragg}} = 1.54$, $R_{\text{F}} = 1.61$	$\text{Tb}^{(1)}\text{-6h}$	0.238(1)	0.228(2)	1/4	0.87	1.0
	$\text{Tb}^{(2)}\text{-6h}$	0.511(3)	0.130(1)	1/4	1.02	1.0
	$\text{Co}^{(1)}\text{-2b}$	0	0	0	0.60	0.26(5)
	$\text{Co}^{(2)}\text{-2c}$	1/3	2/3	1/4	0.63	1.0
	$\text{Co}^{(3)}\text{-4e}$	0	0	0.167(2)	0.60	0.20(5)
	Si-6h	0.168(2)	0.456(5)	1/4	1.01	1.0
	$\text{D}^{(1)}\text{-4f}$	1/3	2/3	0.629(5)	3.51	0.49(3)
	$\text{D}^{(2)}\text{-12i}_1$	0.423(4)	0.385(3)	0.502(6)	3.95	0.87(8)
	$\text{D}^{(3)}\text{-12i}_2$	0.203(2)	0.358(3)	0.496(4)	2.11	0.83(6)
		0	0.132(1)	1/4	0.6	1.0
		0	0.401(5)	1/4	1.0	1.0
$\text{TbNiD}_{3.3}$ Space group Cmcm $a = 3.740(2)$ $b = 11.435(6)$ $c = 4.671(3)$ $V = 199.8(3)$ ($\Delta V/V_0 = 23.4\%$) $R_{\text{Bragg}} = 1.28$, $R_{\text{F}} = 1.81$	Tb-4c	0	0.132(1)	1/4	0.6	1.0
	Ni-4c	0	0.401(5)	1/4	1.0	1.0
	$\text{D}^{(1)}\text{-8f}$	0	0.307(5)	0.497(7)	2.1	1.0
	$\text{D}^{(2)}\text{-4c}$	0	0.920(2)	1/4	2.7	1.0
	$\text{D}^{(3)}\text{-4b}$	0	1/2	0	2.1	0.32(1)
$\text{DyNiD}_{3.3}$ Space group Cmcm $a = 3.719(2)$ $b = 11.329(5)$ $c = 4.645(2)$ $V = 195.7(2)$ ($\Delta V/V_0 = 22.4\%$) $R_{\text{Bragg}} = 2.07$, $R_{\text{F}} = 1.51$	Dy-4c	0	0.133(2)	1/4	1.02	1.0
	Ni-4c	0	0.408(7)	1/4	1.06	1.0
	$\text{D}^{(1)}\text{-8f}$	0	0.303(4)	0.511(7)	2.38	1.0
	$\text{D}^{(2)}\text{-4c}$	0	0.929(1)	1/4	2.41	1.0
	$\text{D}^{(3)}\text{-4b}$	0	1/2	0	2.43	0.38(1)

* Isotropic Debye-Waller factor.

R–M distances increase insignificantly. This is due to the fact that the expansion of the R_3 face in the ab plane is accompanied by the reduction of the tetrahedron height owing to the cell contraction along the z axis. The introduction of deuterium atoms into the $12i_1$ and $12i_2$ sites causes an anisotropic distortion of these interstices. Two R–R distances in the tetrahedron face R_3 increase by 3–4%, and the third distance increases by 6–7%. Likewise, one R–Si distance increases by 7–8%, whereas the two other R–Si distances increase insignificantly (by $\sim 1\%$).

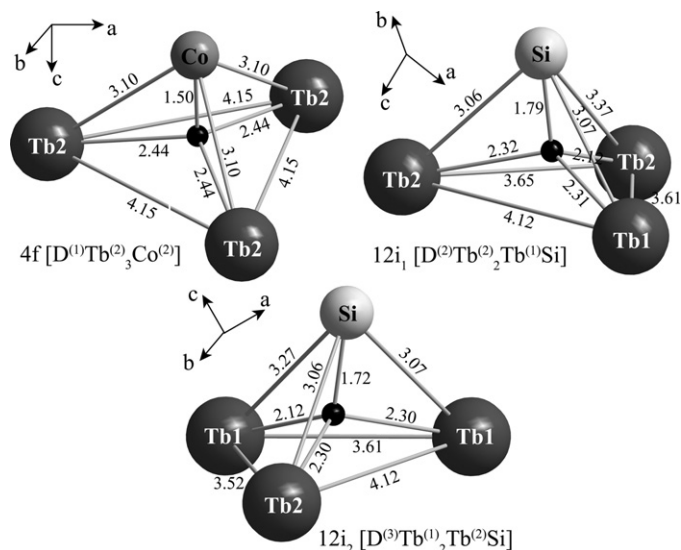


Fig. 3. Coordination polyhedra of deuterium atoms in the $4f\text{-}[\text{D}^{(1)}\text{Tb}_3\text{Co}]$, $12i_1\text{-}[\text{D}^{(2)}\text{Tb}_2\text{Si}]$ and $12i_2\text{-}[\text{D}^{(3)}\text{Tb}_2\text{Si}]$ sites of the $\text{Tb}_6\text{Co}_{1.67}\text{Si}_3\text{D}_{11.2}$ structure.

The R–D and T–D distances in the structures of $\text{Tb}_6\text{Co}_{1.67}\text{Si}_3\text{D}_{11.2}$ and $\text{Ce}_6\text{Ni}_{1.67}\text{Si}_3\text{D}_{12.3}$ are similar to the distances observed in other IMCs of the respective rare earth metals. These hydrides have interatomic distances typical of the binary hydrides of the constituent metals. A similar situation was previously discussed for transition metal IMC hydrides [17,18]. The D–Si distances in the structure of $\text{Ce}_6\text{Ni}_{1.67}\text{Si}_3\text{D}_{12.3}$ are close to the corresponding distance in the structure of $\text{CeNiSiD}_{1.2}$ (2.02 \AA [19]). They are longer than the Si–H bond lengths reported for different silicon-based compounds with a largely covalent bonding between the hydrogen and silicon atoms ($d_{\text{cov}} = 1.48 \text{ \AA}$). In the structure of $\text{Tb}_6\text{Co}_{1.67}\text{Si}_3\text{D}_{11.2}$, these interatomic distances are slightly shorter ($1.72\text{--}1.79 \text{ \AA}$). We think that the difference between the Si–H bond lengths in the above compounds and CaSiD_{1+x} [20] is mainly due to the difference between the atomic radii of the metal atoms. In addition, CaSi is a pure silicide phase with a higher silicon content and another arrangement of the Si atoms. For this reason, we assume that the D–Si distances obtained in this study are quite reasonable and are indeed longer than the Si–H bonds reported for silicon-based compounds with largely covalent hydrogen–silicon bonding.

3.2. Crystal structure of $\text{TbNiD}_{3.3}$ and $\text{DyNiD}_{3.4}$

According to our X-ray diffraction data, the RNi compounds have a CrB-type orthorhombic structure, space group Cmcm (GdNi, SmNi); a FeB-type structure, space group Pnma (DyNi); or a low-temperature TbNi-type monoclinic structure, space group $\text{P2}_1/m$ (TbNi) in agreement with results in the literature [21,22]. Irrespective of the crystal structure of the RNi compounds, their hydrides have a CrB-type structure. DyNi and TbNi undergo a structural transformation upon hydrogenation, turning into another structure type. The hydrogenation of GdNi and SmNi is accompanied by

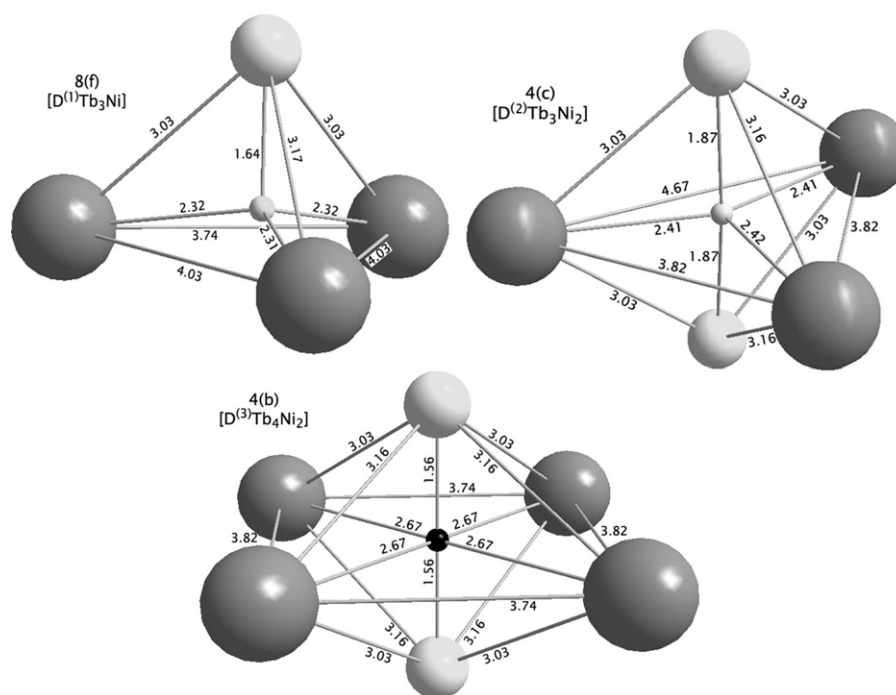


Fig. 4. Coordination polyhedra of deuterium atoms in the 8f-[D⁽¹⁾R₃Ni], 4c-[D⁽²⁾R₃Ni₂] and 4b-[D⁽³⁾R₄Ni₂] sites of the TbNiD_{3.3} structure.

anisotropic lattice expansion without reordering the metal sublattice.

Neutron powder diffraction measurements for TbNiD_{3.4} and DyNiD_{3.4} were performed to determine the deuterium atom positions and their occupancies. The data obtained were used to refine the structure parameters (Table 1) and interatomic distances. The calculated deuterium contents of the hydride phases corresponded to the formulas TbNiH_{3.3} and DyNiH_{3.4}. The difference between the deuterium content values calculated for TbNiH_{3.3} by different methods (volumetric data and deuterium site occupancies) can be due to the partial desorption of deuterium from the sample after decompression. The estimated accuracy of the D/f.u. determination from the neutron diffraction data is 3%.

An analysis of the neutron diffraction patterns revealed three types of interstices occupied by deuterium atoms: 4c, 8f and 4b (Table 1, Fig. 4). This structural model was earlier reported for the ternary deuteride LaNiD_{3.7} [23]. The coordination polyhedron of a

deuterium atom is a distorted trigonal bipyramid 4c-[R₃Ni₂], distorted tetrahedron 8f-[R₃Ni], and distorted octahedron 4b-[R₄Ni₂], respectively. A coordination polyhedron analysis shows that deuterium atoms should successively occupy interstices in the order of increasing coordination number: first the tetrahedral sites, then trigonal bipyramidal sites, and finally octahedral interstices. As in other superstoichiometric hydrides (D/f.u. > 3), the occupation of the octahedral 4b-sites begins after the complete filling of the 4c and 8f interstices.

3.3. Magnetic properties of the deuterides

The compounds Gd₆Ni_{1.67}Si₃, Gd₆Co_{1.67}Si₃, and Tb₆Co_{1.67}Si₃ are ferromagnetic materials with Curie temperatures of, respectively, T_C = 305, 298, and 178 K (Table 2) determined from the temperature dependences of magnetization.

Table 2

Crystallographic and magnetic data for the IMCs and their hydrides.

Compound	Structure type	Unit cell parameters (Å)	μ_{eff}^* (μ_{B})	T _C ** (K)	$\theta_{\text{p}}^{\text{***}}$ (K)
GdNi	CrB	$a = 3.778(4)$, $b = 10.337(6)$, $c = 4.238(5)$	8.3	–	80
GdNiH _{3.2}	CrB	$a = 3.767(2)$, $b = 11.576(7)$, $c = 4.733(3)$	7.5	–	21
TbNi	TbNi	$a = 21.31(2)$, $b = 4.211(4)$, $c = 5.454(2)$, $\beta = 97.43^\circ$	10.0	–	56
TbNiH _{3.4}	CrB	$a = 3.740(2)$, $b = 11.435(6)$, $c = 4.671(3)$	10.3	–	–12
DyNi	FeB	$a = 7.025(4)$, $b = 4.181(3)$, $c = 5.445(2)$	10.3	–	51
DyNiH _{3.4}	CrB	$a = 3.719(2)$, $b = 11.329(5)$, $c = 4.645(2)$	10.1	–	3
SmNi	CrB	$a = 3.782(3)$, $b = 10.375(4)$, $c = 4.301(2)$	–	–	–
SmNiH _{3.7}	CrB	$a = 3.791(2)$, $b = 11.644(4)$, $c = 4.761(2)$	–	–	–
Ce ₆ Ni _{1.67} Si ₃	Ce ₆ Ni ₂ Si ₃	$a = 12.071(3)$, $c = 4.312(1)$	–	–	–
Ce ₆ Ni _{1.67} Si ₃ H _{12.3}	Ce ₆ Ni ₂ Si ₃	$a = 13.00(2)$, $c = 4.134(3)$	–	–	–
Gd ₆ Ni _{1.67} Si ₃	Ce ₆ Ni ₂ Si ₃	$a = 11.736(6)$, $c = 4.180(2)$	6.4	305	13
Gd ₆ Ni _{1.67} Si ₃ H _{12.3}	Ce ₆ Ni ₂ Si ₃	$a = 12.44(2)$, $c = 3.983(8)$	–	–	–
Gd ₆ Co _{1.67} Si ₃	Ce ₆ Ni ₂ Si ₃	$a = 11.76(1)$, $c = 4.161(4)$	7.0	298	29
Gd ₆ Co _{1.67} Si ₃ H _{12.6}	Ce ₆ Ni ₂ Si ₃	$a = 12.54(1)$, $c = 3.970(3)$	–	–	–
Tb ₆ Co _{1.67} Si ₃	Ce ₆ Ni ₂ Si ₃	$a = 11.685(6)$, $c = 4.136(2)$	8.5	178	196
Tb ₆ Co _{1.67} Si ₃ H _{11.2}	Ce ₆ Ni ₂ Si ₃	$a = 12.353(7)$, $c = 3.950(3)$	8.6	–	15

* Effective magnetic moment per a rare earth atom; μ_{B} is Bohr magneton.

** Curie temperature.

*** Paramagnetic Curie temperature.

The hydrogenation of the $R_6M_{1.67}Si_3$ compounds leads to the weakening of the ferromagnetic interaction and to a decrease in the magnetic transition temperature. A similar effect was observed for the $RNi-H_2$ systems [10]. The calculated paramagnetic Curie temperatures are $\theta_p = 13, 29,$ and 15 K for $Gd_6Ni_{1.67}Si_3H_{12.3}$, $Gd_6Co_{1.67}Si_3H_{12.6}$ and $Tb_6Co_{1.67}Si_3H_{11.2}$, respectively. The calculated effective magnetic moments are close to the data reported by other authors [13,15,22] and to the magnetic moments of the free rare earth ions. In addition, the influence of hydrogen on the magnetic moments is negligible. Therefore, the 3d-bands of nickel and cobalt are filled in these compounds and the observed magnetization is solely due to the magnetic moments of the rare earth atoms.

The 4f–4f exchange interactions between rare earth atoms decrease with increasing R–R distance. In spite of the very anisotropic lattice distortion, all R–R distances in the $R_6M_{1.67}Si_3$ compounds increase upon hydrogenation. Although the unit cell contracts along the z axis, the lattice expansion in the xy plane leads to the increase in all interatomic distances. Neutron diffraction data revealed a hydrogen-induced increase in the interatomic distances in RNi and $R_6M_{1.67}Si_3$ compounds, too. Thus, the decrease in the magnetization and magnetic transition temperature of these compounds upon hydrogenation mainly results from the weakening of the 4f–4f exchange interaction caused by the lattice expansion.

4. Conclusions

The intermetallic compounds RNi ($R = Gd, Tb, Dy, Sm$) and $R_6M_{1.67}Si_3$ ($R = Ce, Gd, Tb; M = Ni, Co$) interact readily with hydrogen at room temperature and hydrogen pressures of up to 1.0 MPa. The hydrides of the RNi compounds have a CrB-type orthorhombic structure. The $R_6M_{1.67}Si_3$ compounds retain their $Ce_6Ni_2Si_3$ -type structure upon hydrogenation. In spite of the very anisotropic distortion of their crystal lattices, all of the hydrides demonstrate increased interatomic distances in comparison with their parent IMCs. The lattice expansion results in a substantial decrease in the exchange interaction strength and in the magnetic transition

temperature. The effective magnetic moments of the compounds remain unchanged upon hydrogenation.

Acknowledgment

The authors thank Dr. V.A. Somenkov for his critical reading of the paper and helpful discussions and comments.

References

- [1] V.K. Pecharsky, K.A. Gschneidner, Phys. Rev. Lett. 78 (1997) 4494–4497.
- [2] A.V. Deryagin, V.N. Moskalev, N.V. Mushnikov, S.V. Terentyev, Phys. Met. Metallogr. 57 (1984) 1086.
- [3] S.A. Nikitin, I.S. Tereshina, V.N. Verbetsky, A.A. Salamova, J. Alloys Compd. 1–2 (316) (2001) 46–50.
- [4] I.S. Tereshina, S.A. Nikitin, V.N. Verbetsky, A.A. Salamova, J. Alloys Compd. 336 (2002) 36–40.
- [5] S.A. Nikitin, I.S. Tereshina, Phys. Solid State 10 (45) (2003) 1944–1951.
- [6] S.K. Tripathy, K.G. Suresh, R. Nirmala, A.K. Nigam, S.K. Malik, Solid State Commun. 5 (134) (2005) 323–327.
- [7] P. Kumar, K.G. Suresh, A.K. Nigam, O. Gutfleisch, J. Phys. D: Appl. Phys. 41 (2008) 245006.
- [8] Shen Jun, Li Yang-Xian, Dong Qiao-Yan, Wang Fang, Sun Ji-Rong, Chin. Phys. B 6 (17) (2008) 2268–2271.
- [9] Jun Shen, Fang Wang, Yang-Xian Li, Ji-Rong Sun, Bao-Gen Shen, J. Alloys Compd. 458 (2008) L6–L8.
- [10] Yu.L. Yaropolov, V.N. Verbetsky, A.S. Andreenko, K.O. Berdyshev, S.A. Nikitin, Inorg. Mater. 46 (2010) 364–371.
- [11] O.I. Bodak, E.I. Gladyshevsky, O.I. Kharchenko, Crystallogr. Rep. 1 (19) (1974) 80–83.
- [12] E. Gaudin, B. Chevalier, J. Solid State Chem. 180 (2007) 1397–1409.
- [13] B. Chevalier, E. Gaudin, F. Weill, J. Alloys Compd. 442 (2007) 149–151.
- [14] E. Gaudin, S. Tence, B. Chevalier, Solid State Sci. 10 (2008) 481–485.
- [15] E. Gaudin, S. Tence, F. Weill, J. Fernandez, B. Chevalier, Chem. Mater. 9 (20) (2008) 2972–2979.
- [16] V.A. Yartys', V.V. Burnasheva, K.N. Semenenko, N.V. Fadeeva, S.P. Solov'ev, Int. J. Hydrogen Energy 12 (7) (1982) 957–965.
- [17] V.A. Somenkov, S.Sh. Shilstein, Z. Phys. Chem. 117 (1979) 125–144.
- [18] V.A. Somenkov, A.V. Irodova, J. Less-Common Met. 101 (1984) 481–492.
- [19] M. Pasturel, F. Weill, F. Bouree, J.-L. Bobet, B. Chevalier, J. Alloys Compd. 397 (2005) 17–22.
- [20] H. Wu, W. Zhou, T.J. Udovic, J.J. Rush, T. Yildirim, Phys. Rev. B: Condens. Matter 74 (2006) 224101.
- [21] R. Lemaire, D. Paccard, J. Less-Common Met. 4 (21) (1970) 403–413.
- [22] R.E. Walline, W.E. Wallace, J. Chem. Phys. 6 (41) (1964) 1587–1591.
- [23] V.V. Burnasheva, V.A. Yartys', N.V. Fadeeva, S.P. Solov'ev, K.N. Semenenko, Acta Crystallogr. Sect. A: Found. Crystallogr. 37 (1982) C182.